

Aus der Abteilung für Biosynthese Neuraler Strukturen
des Zentrums für Molekulare Neurobiologie
des Universitätskrankenhaus Hamburg-Eppendorf
Direktorin Frau Prof. Dr. M. Schachner

Quantitative Morphological Analyses of the striatum and
cerebellum of Tenascin-R deficient mice

D i s s e r t a t i o n

zur Erlangung des Grades eines Doktors der Medizin dem
Fachbereich Medizin der Universität Hamburg vorgelegt von

Ann – Britt Steen

aus Stade

Hamburg 2006

Angenommen vom Fachbereich Medizin
der Universität Hamburg am: 27.10.2006

Veröffentlicht mit Genehmigung des Fachbereichs
Medizin der Universität Hamburg

Prüfungsausschuss, der/die Vorsitzende: Prof. Dr. M. Schachner

Prüfungsausschuss: 2. Gutachter/in: Prof. Dr. M. Davidoff

Prüfungsausschuss: 3. Gutachter/in: Prof. Dr. O. Pongs

CONTENT

1 INTRODUCTION	3
1.1 Tenascin-R	3
1.1.1 General	3
1.1.2 Structure	4
1.1.3 Function	5
1.2 Tenascin-R-deficient Mouse	7
1.2.1 Morphology	7
1.2.2 Physiology	8
1.2.3 Behaviour	10
1.2.4 Motor Coordination	10
1.3 Tenascin-R in humans	10
2 RATIONALE AND AIMS OF THE STUDY	12
3 MATERIAL AND METHODS	14
3.1 Animals	14
3.2 Preparation of tissue for sectioning	14
3.3 Preparation of cryostat sections	15
3.4 Stereological analysis of immunohistochemically defined cell types	16
3.4.1 Antibodies	16
3.4.2 Immunohistochemical stainings	16
3.4.3 Stereological analysis	17
3.4.4 Estimation of volume of striatum and layer thickness in the cerebellum	19
3.4.5 Photographic documentation	20
3.4.6 Statistical analysis	20
4 RESULTS	21
4.1 Immunohistochemical markers, quality of staining and qualitative observations in TN-R+/+ and TN-R-/- animals	21
4.2 Stereological Analyses of the Striatum	24
4.2.1 Volume of the Striatum	24
4.2.2 Total cell density	24
4.2.3 Total neuronal population	25
4.2.4 Interneurons	26
4.2.4.1 Parvalbumin-positive interneurons	26
4.2.4.2 Cholinergic interneurons of the striatum	27
4.2.5 Glial cells	28
4.2.5.1 Oligodendrocytes	28
4.2.5.2 Astrocytes	29
4.2.5.3 Microglia	30
4.3 Stereological Analyses of the Cerebellum	31
4.3.1 Thickness of the molecular layer and the granular layer	31
4.3.2 Total neuronal population of the granular layer	33
4.3.3 Interneurons	33
4.3.3.1 Parvalbumin-positive interneurons (basket, stellate and Golgi cells)	33
4.3.3.2 Purkinje neurons	34
4.3.3.3 Ratio Purkinje cells / interneurons (basket, stellate and Golgi cells)	35

4.3.4 Glial cells	36
4.3.4.1 Oligodendrocytes in the granular layer	36
4.3.4.2 Astrocytes in the cerebellum.....	37
4.3.4.3 Microglia.....	38
5 DISCUSSION.....	39
5.1 Genotype-related aberrations in adult mice.....	40
5.2 Genotype-related aberrations in old mice	43
5.3 Age-related changes.....	44
5.4 Possible functional significance of the structural aberrations in TN-R deficient mice.....	46
6 SUMMARY	47
7 REFERENCES	50
8 ABBREVIATIONS:	56
9 ACKNOWLEDGMENTS	59
10 CURRICULUM VITAE	60
11 EIDESSTATTLICHE VERSICHERUNG.....	61

1 INTRODUCTION

1.1 Tenascin-R

1.1.1 General

Tenascin-R (TN-R) is an extracellular matrix (ECM) glycoprotein which is restricted to the central nervous system (CNS) (Bartsch et al. 1993; Pesheva et al. 1989). It is a member of the tenascin family together with tenascin-C (TN-C), tenascin-X (TN-X), tenascin-Y (TN-Y) and tenascin-W (TN-W) (Jones and Jones 2000). Glycoproteins of this family display highly restricted and dynamic patterns of expression in the embryo, particularly during neural development, skeletogenesis, and vasculogenesis. In the adult, these molecules are re-expressed during wound healing, nerve regeneration, tissue involution, vascular diseases, tumorigenesis and metastasis. TN-R is found in diverse species from zebrafish to human. It is found in two major molecular isoforms: one isoform of 160kD (kilo Dalton) which forms both monomers and dimers (J1-160) and a second form of 180kD that forms trimers (J1-180) (Bartsch et al. 1993; Pesheva et al. 1989; Fuss et al 1993). Other names in older studies are janusin (J1-160/180) or restrictin.

TN-R is synthesised by oligodendrocytes with high expression during myelination (Bartsch et al. 1993; Wintergerst et al. 1993). It is also synthesised by subpopulations of neurons such as horizontal cells in the retina, Purkinje, stellate and basket cells in the cerebellum, motoneurons in the spinal cord and some neurons in the hippocampus (Bartsch et al. 1993; Fuss et al. 1993; Wintergerst et al. 1993; Woodworth et al. 2002; Becker et al. 2003). Furthermore, it is associated with nodes of Ranvier (Bartsch et al. 1993). It is

found on unmyelinated and myelinated axons, on oligodendrocytes and on outer aspects of myelin sheaths in adult animals (Bartsch et al. 1993). The expression of tenascin-R in oligodendrocytes is influenced by co-culture with astrocytes and neurons, while astrocytes elevated the expression of tenascin-R by oligodendrocytes and neurons decreased the expression of tenascin-R by oligodendrocytes (Jung et al. 1993).

Immunohistochemical analysis of TN-R expression in the adult rat brainstem has revealed two main locations: (1) in the neuropil where it is diffusely distributed and (2) in perineuronal nets around motoneuron somata (Angelov et al. 1998). TN-R expression in perineuronal nets is also prominent in other areas of the CNS such as hippocampus, occipital cortex, medial globus pallidus and cerebellar nuclei (examples) (Bruckner et al. 2000).

1.1.2 Structure

The amino acid sequence of TN-R has been well preserved during evolution. For example, in zebrafish the complete open reading frame of TN-R encodes a deduced protein of 1351 amino acids the sequence of which is about 60% identical to those of tenascin-R in chicken, human and rat (Becker et al. 2003). TN-R shares varying degrees of similarity also with the other members of the tenascin family (Erickson 1993). TN-R has a Tenascin Assembly (TA) domain, which containing cysteine residues and three to four α -helical heptad repeats, that enable formation of dimers and trimers (Fuss et al. 1993; Erickson 1994; Jones and Jones 2000). TN-R contains also 4.5 epidermal growth factor (EGF)-like domains that play key roles in neuronal migration and axon pathfinding during development. Eight or nine fibronectin (FN) type III-like

domains allow binding to several ligands including other ECM proteins, glycosaminoglycans and a number of different cell surface receptors. A fibrinogen globe that can bind Ca^{2+} is involved in interactions with cell surface receptors or other matrix molecules. The structure of TN-R is shown in Fig. 1.

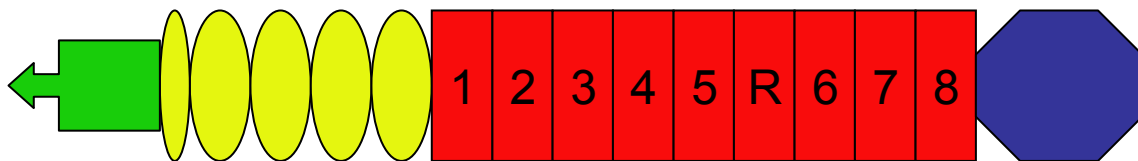


Figure 1: The structure of tenascin-R. Shown are the Tenascin Assembly domain (green), the epidermal growth factor-like domains (yellow), the fibronectin type III-like domains (red) and the fibrinogen globe (blue).

1.1.3 Function

The functions of TN-R are multiple. It is needed for the correct assembly of neuronal nets together with other glycoproteins like tenascin-C, chondroitin-sulfate proteoglycans, phosphacan or lecticans like brevican and versican (Haunso et al. 2000; Celio and Blümcke 1994; Celio and Chiquet-Ehrismann 1993; Bruckner et al. 2000; Hagihara et al. 1999; Angelov et al. 1998; Weber et al. 1999). Neuronal nets were a specialized form of extracellular matrix, which surround the cell bodies and the proximal dendrites of some excitatory neurons (e.g., motoneurons) and parvalbumin-positive interneurons (the main subpopulation of GABAergic neurons) in the adult central nervous system (Celio and Blümcke 1994; Weber et al. 1999) where TN-R and brevican show remarkable colocalization (Hagihara et al. 1999).

TN-R supports the adhesion of and process formation by oligodendrocytes *in vitro* (Pesheva et al. 1997). TN-R may, however, both inhibit and promote neurite outgrowth by neurons depending on cell type and on the way it is presented to the cells, i.e. as an uniform substrate or substrate boundary (Pesheva et al. 1994; Schachner 1994; Schachner et al. 1994; Faissner 1997; Becker et al. 2000). For example, when TN-R is offered as a sharp substrate boundary with tenascin-C, growth cone neurons of both retinal and dorsal root ganglion cells avoid growing on this substrate but do not collapse (Taylor et al. 1993). However, when TN-R and TN-C are offered in a mixture with laminin as an uniform substrate, dorsal root ganglion neurons collapse and are able to advance at a faster rate than on laminin alone. In contrast, the outgrowth of retinal ganglion neuron growth cones is completely inhibited when offered an uniform substrate of TN-R and TN-C with laminin. Furthermore, TN-R is adhesive or repulsive to different cell types at the same time. This dual response is depending on the partner cell type and on the time of interaction (Morganti et al. 1990; Pesheva et al. 1993; Schachner et al. 1994). The first phase of interaction (shorter than 1 hour) seems to be adhesive and thereafter it seems to be repulsive. The dual quality of TN-R-mediated interaction appears to be characteristic of neurons.

TN-R is anti-adhesive for activated microglia and it is down-regulated in the facial motor nucleus after peripheral nerve injury (Angelov et al. 1998).

TN-R can bind to several other extracellular matrix molecules, for example CALEB (chicken acidic leucine-rich EGF-like domain containing brain protein) or fibronectin (Schumacher et al. 2001; Schumacher and Stübe 2003; Pesheva et al. 1994). TN-R binds also to a chondroitin sulphate proteoglycan

(CSPG) related to phosphacan, isolated from mouse brain and thereby modulate its inhibitory influence on neuritogenesis (Xiao et al. 1997). Another important binding partner of TN-R is the cell surface receptor F3/F11 (Pesheva et al. 1993). TN-R binds to the voltage-gated sodium channel via its fibronectin (FN) domains 1-2 and 6-8 and its EGF-domains and modulates the channel function (Srinivasan et al. 1998; Xiao et al. 1999). TN-R carries an unusual glycan, the HNK-1 carbohydrate, via which it modulates perisomatic inhibition and long-term potentiation in the CA1 region of the hippocampus (Saghatelian et al. 2000).

TN-R associated with Purkinje cell bodies and their dendrites in the molecular layer of the cerebellum bears *N*-linked oligosaccharides terminating with β 1,4-linked GalNAc-4-SO₄, whereas TN-R in other regions of the cerebellum did not bear this modification (Woodworth et al. 2002). The expression of this unique sulphated carbohydrate structure is temporally regulated. It is increased during cerebellum development mostly between postnatal day 14 and 21, corresponding to a period of Purkinje cell dendrite extension and synaptogenesis.

1.2 Tenascin-R-deficient Mouse

1.2.1 Morphology

Only a few structural abnormalities have been reported up to now for mice deficient in the expression of TN-R. The gross-anatomical appearance of the TN-R deficient mouse is normal (Weber et al. 1999; Haunso et al. 2000). Young TN-R deficient mice have normal body weight but at the age of 11

months they become slightly heavier than wild-type littermates (Freitag et al. 2003). The perineuronal nets are abnormal: the net structure is disorganized, with a punctate appearance; and the primary dendritic shafts are, in contrast to wild-type mice, barely unsheathed by nets (Weber et al. 1999). In the hippocampus, TN-R deficient mice have lower numbers of calretinin-positive neurons and more glial fibrillary acidic protein (GFAP)-immunoreactive astrocytes compared to wild-type littermates (Brenneke et al. 2004). Abnormalities in perisomatic synapses in the hippocampus of TN-R deficient mice have also been reported (Nikonenko et al. 2003, see 1.2.2 below).

1.2.2 Physiology

Abnormalities in synaptic transmission and plasticity in the hippocampus have been detected by electrophysiological measurements in TN-R deficient (TN-R^{-/-}) mice. NMDA (*n*-methyl-D-aspartate) receptor-dependent long-term potentiation (LTP) is reduced in the CA1 region of the hippocampus (Saghatelian et al. 2001). Basal excitatory synaptic transmission in synapses formed on CA1 pyramidal cell bodies is increased and the amplitude of unitary inhibitory postsynaptic currents (IPSC) evoked by stimulation of perisomatic interneurons is reduced by a factor of two. The frequency of failures in γ -aminobutyric acid (GABA) release is increased. Additionally, mice deficient in the glycoprotein TN-R have a reduced perisomatic inhibition. The reduction of the LTP induced by theta-burst stimulation of Schaffer collaterals of the stratum radiatum is two-fold smaller in TN-R deficient compared with wild-type mice (Bukalo et al. 2001). Upon repetitive stimulation of Schaffer collaterals at 1Hz, the numbers of secondary spikes are significantly increased in the stratum

radiatum of the CA1 region in the hippocampus of TN-R deficient mice (Brenneke et al. 2004). Another physiological abnormality identified in TN-R deficient mice is reduced conduction velocity of optic nerve fibres (Weber et al. 1999).

Aberrations in symmetric perisomatic (putatively inhibitory) synapses in the CA1 region of the hippocampus of TN-R deficient mice have been identified as likely morphological substrates of abnormal inhibition (Nikonenko et al. 2003). The perisomatic coverage of the principle neurons with active zones is reduced by more than 40% and individual active zones are smaller than in wild-type mice. In addition, the spatial arrangement of pyramidal cell bodies is a more diffuse in TN-R mice compared with wild-type littermates.

In vivo recordings have shown that TN-R deficient mice have multiple abnormalities in the hippocampal electroencephalographic (EEG) activity and in auditory-evoked responses in the hippocampus and the cortex (Gurevicius et al. 2004). Normally, the CA1 layer of the hippocampus is characterized by high-frequency ripple oscillations. These oscillations are not altered in TN-R^{-/-} mice. However, the theta rhythm is moderately decreased in frequency with no change in the amplitude and the amplitude of the gamma waves is strongly increased in TN-R^{-/-} mice. The amplitudes of all components of the auditory-evoked potentials (AEPs) in the cortex are increased. In the hippocampal recordings only the early components of the AEPs have higher amplitudes in TN-R^{-/-} compared with wild-type mice (Gurevicius et al. 2004).

1.2.3 Behaviour

Behavioural abnormalities have also been observed in TN-R deficient mice. In the open field test, TN-R deficient mice move and explore less and avoid staying in the centre of the arena indicating increased state and trait anxiety (Freitag et al. 2003). Aggressive behaviour of TN-R deficient mice is similar to that of wild-type animals.

1.2.4 Motor Coordination

The TN-R deficient mice perform poorly in motor coordination tests such as pole, wire-hanging and rotarod tests (Freitag et al. 2003; Montag-Sallaz and Montag 2003). In the pole test, TN-R deficient mice are not able, in contrast to wild-type littermates, to turn 180° and climb down with head pointing downwards. However, the mutant mice are able to improve their performance during three consecutive trials. Coordination in space, as seen in the wire-hanging test, is also impaired since mutant mice are not able to lift their body and grasp the wire with their hind paws. The TN-R deficient mice are able to stay on the accelerating Rotarod for shorter time-periods compared with wild-type mice.

1.3 Tenascin-R in humans

TN-R is widely expressed in the central nervous system of humans. It is present found both in the white and grey matter of the cerebrum, in contrast to TN-C which is expressed only in the white matter. In the cerebellum and the spinal cord TN-R is also observed in both the white matter as in the grey matter

but here the expression in the grey matter is higher (Gutowski et al. 1999). The gene encoding TN-R is localized on chromosome 1 in the locus 1q23-1q24 (Carnemolla et al. 1995).

2 RATIONALE AND AIMS OF THE STUDY

Different behavioural and physiological abnormalities have been identified so far in TN-R deficient mice. The morphological substrates of these anomalies are unknown with one exception: alterations in perisomatic inhibitory synapses can explain decreased hippocampal inhibition (Nikonenko et al. 2003). One of the most prominent features in the phenotype of the TN-R deficient mouse is the impairment of motor control. This study was designed to address the question of the structural basis of this impairment. Two brain areas were selected for analysis: the cerebellum and the neostriatum (referred to, for simplicity, as striatum throughout the text). These brain structures are of particular importance for control of movement and posture and execution of motor programmes (Trepel 1995). The methodological approach applied in the study was that of Irintchev et al. 2005. It is based on immunohistochemical visualization of defined cell types such as total neuronal population, subpopulations of interneurons, astrocytes, oligodendrocytes and microglia, and stereological estimation of cell densities and volumes of structures. The numerical data produced by this approach allow in-depth characterization of a given brain structure. The particular aims of these investigations were to determine whether:

1. TN-R deficiency causes changes in the gross structure (volume) of the cerebellum and striatum;
2. major cell populations are normally formed and maintained in size throughout life in the absence of TN-R.

In order to answer the second question, both adult (5 months of age) and old (18-20 months) TN-R deficient mice and wild-type littermates were included in the analyses.

3 MATERIAL AND METHODS

3.1 Animals

Eight wild-type (TN-R+/+) mice and eight TN-R-deficient (TN-R-/-) littermates were studied at the age of 5 months (Mo)(adult mice). Six animals per genotype were analysed at the age of 18 – 20 months (old mice). The TN-R deficient animals have a C57BL/6J x 129Ola genetic background (Weber et al. 1999). The animals were bred in the SPF (specific pathogen-free) facility of the Universitätsklinikum Hamburg (UKE). All animals appeared healthy before sacrifice for morphological analyses. Mean body weight was similar in TN-R deficient and wild-type mice: 32 ± 3.3 g *versus* 33 ± 3.2 g and 32 ± 3.6 g *versus* 34 ± 5.5 g in TN-R+/+ *versus* TN-R-/- animals studied at the age of 5 and 18 months, respectively ($p > 0.05$, two-sided *t* tests for independent groups). The genotype of the mutant mice had been determined in advance by polymerase chain reaction (PCR, Weber et al. 1999). Animal treatments were performed in accordance to the German law for protection of experimental animals. All technical procedures described below were performed according to Irintchev et al. 2005.

3.2 Preparation of tissue for sectioning

Mice were weighed and anaesthetised with 16% solution of sodium pentobarbital (Narcofen, Merial, Hallbergmoos, $5 \mu\text{l g}^{-1}$ body weight, i.p.). After surgical tolerance was achieved, the animals were transcordially perfused with physiologic saline for 60 seconds followed by fixative consisting of 4%

formaldehyde and 0.1% CaCl₂ in 0.1M cacodylate buffer, pH 7.3, for 15 minutes at room temperature (RT). Following perfusion the brains were left *in situ* for 2 hours at RT to reduce fixation artefacts after which they were dissected out without the olfactory bulbs and post-fixed overnight (18-20 hours) at 4°C in the formaldehyde solution used for perfusion. The tissue was then immersed for two days in 15% sucrose solution in 0.1M cacodylate buffer, pH 7.3, at 4°C.

Fixed and cryoprotected (sucrose-infiltrated) brains were carefully examined under a stereomicroscope and hair, rests of dura mater or other tissue debris were removed with a fine forceps. Afterwards, the brains were placed in a mouse brain matrix (World Precision Instruments, Berlin) and the caudal end was cut at a defined level (1mm from the most caudal slot of the matrix). Finally the brains were frozen by inserting into 2-methyl-butan (isopentan) precooled to -30°C in the cryostat for 2 minutes. The brains were stored in liquid nitrogen until sectioned.

3.3 Preparation of cryostat sections

For sectioning, the caudal pole of each brain was attached to a cryostat specimen holder using a drop of distilled water placed on a pre-frozen layer of Tissue Tek (Satura Finetek Europe, Zoeterwoude, The Netherlands). The ventral surface of the brain was oriented to face the cryostat knife edge and serial coronal sections of 25 µm thickness were cut in a cryostat Leica CM3050 (Leica Instruments, Nußloch, Germany). Sections were collected on Super Frost Plus glass slides (Roth, Karlsruhe, Germany). Since stereological analyses require extensive sectioning of the structures under study and use of

spaced-serial sections (Howard and Reed, 1998), sampling was always done in a standard sequence so that 4 sections 250 μm apart were presented on each slide.

3.4 Stereological analysis of immunohistochemically defined cell types

3.4.1 Antibodies

The following commercially available antibodies were used at optimal dilutions: anti-parvalbumin (PV, mouse monoclonal, clone PARV-19, Sigma, Deisenhofen, Germany, dilution 1:1000), anti-neuron specific nuclear antigen (NeuN, mouse monoclonal, clone A60, Sigma, 1:1000), anti-cyclic nucleotide phosphodiesterase (CNPase, mouse monoclonal, clone 11-5B, Sigma, 1:1000), anti-S-100 (rabbit polyclonal, purified Ig G fraction, DakoCytomation, Hamburg, Germany, 1:500), anti-ChAT (goat polyclonal, Chemcon International, Hofheim, Germany, 1:100), and anti-Iba-1 (rabbit polyclonal, affinity purified, Wako Chemicals, Neuss, Germany, 1:1500 0.3).

3.4.2 Immunohistochemical stainings

Sections, stored at -20°C , were air-dried for 30 minutes at 37°C . A 10 mM sodium citrate solution (pH 9.0, adjusted with 0.1 M NaOH) was prepared and preheated in a jar to 80°C in a water bath. The sections were incubated at 80°C for 30 minutes and afterwards the jar was taken out and left to cool down at room temperature. Afterwards, blocking of unspecific binding sites was

performed. The sections were incubated at room temperature for one hour in PBS containing 0.2% Triton X-100 (Fluka, Buchs, Germany), 0.02% sodium azide (Merck, Darmstadt, Germany) and 5% normal goat or donkey serum (Jackson Immuno Research Laboratories, Dianova, Hamburg, Germany). The selection of normal serum for blocking was determined by the species in which the secondary antibody was produced (see below). After one hour the blocking solution was aspirated and the slices were incubated with the primary antibody diluted in PBS containing 0.5% lambda-carrageenan and 0.02% w/v sodium azide in PBS. The slides were incubated for 3 days at 4°C in a screw-cap staining jar (30 ml capacity, Roth). Following this, the sections were washed 3 times in PBS (15 minutes each) before an appropriate (anti-rabbit, anti-mouse or anti-goat) secondary antibody was applied. The sections were incubated with the second antibody diluted (1:200) in PBS-carrageenan at RT for 2 hours. Goat anti-rabbit, goat anti-mouse and donkey anti-goat Ig G conjugated with Cy3 (Jackson Immuno Research Laboratories, Dianova, Hamburg, Germany) were used. After a subsequent wash in PBS, cell nuclei were stained for 10 minutes at room temperature with bis-benzidine solution (Hoechst 33258 dye, 5 µg/ml in PBS, Sigma). Finally, the sections were washed again, mounted with Fluoromount G (Southern Biotechnology Associates, Biozol, Eching, Germany) and stored in the dark at 4°C.

3.4.3 Stereological analysis

The optical dissector method was chosen for quantitative analysis because of its efficiency, an important prerequisite when aiming to quantify numerical densities of a variety of cell types in a given brain region (Irintchev et

al. 2005). The method consists of direct counting of objects in relatively thick sections (e.g., 25 – 50 μm) under the microscope using a three-dimensional counting frame (“counting brick”, see Howard and Reed 1998, referred to here simply as dissector) to “probe” the tissue at random. The base of the frame (dimensions in the x/y plane) is defined by the size of the squares formed by a grid projected into the visual field of the microscope. The height of the dissector is a portion of the section thickness defined by two focus planes in the z axis at a distance of x μm . Control of this parameter is achieved by use of mechanic or electronic devices measuring the movement of the microscope stage in the z axis. Objects (e.g., cells) within each dissector are counted according to stereological rules: Those entirely within the dissector as well as those touching or being dissected by the “acceptance”, but not the “forbidden” planes of the frame are counted (Howard and Reed 1998).

The cell counts were performed on an Axioscope microscope (Zeiss, Oberkochen, Germany) equipped with a motorized stage and NeuroLucida software-controlled computer system (MicroBrightField, Colchester, USA). Sections containing the striatum or the cerebellum were observed under low-power magnification (10 x objective) with a 365/420nm excitation/emission filter set (01, Zeiss, blue fluorescence). The nuclear staining allows delineation of brain structures and areas (Irintchev et al. 2005). The viewed area was randomised by setting a reference point at an arbitrary place resulting in an overlay of the visible field by a grid with lines spaced 30 μm (granular layer of the cerebellum) or 60 μm (all other areas studied) in both axes. The contours of the area of interest were outlined with the cursor. Squares within the marked area 30 μm apart for the granular layer of the cerebellum and 60 μm apart for

the other structures were labelled with a symbol starting from the uppermost left side of the delineated field. A dissector height of 5 μm (granular layer of the cerebellum) or 10 μm (all other areas studied) was chosen since antibody penetration was sufficient to enable clear recognition of stained objects within a depth of at least 15 μm . The sections were then viewed with the 40x objective and 546/590nm excitation/emission filter set (15, Zeiss, red fluorescence) and all marked frames viewed consecutively. Immunolabelled cell profiles that were entirely within the counting frame at any focus level, as well as those attaching to or crossing by the acceptance planes were marked with a symbol. Then, by repeated switching between red and blue filter sets and changing the focus plane, the nuclei of the labelled cells were identified. All nuclei that were in focus beyond a guard space (depth 0-2 μm from the section surface), i.e. lying within 2 and 7 μm (granular layer of the cerebellum) or 2 and 12 μm (all other studies) below the top of the section, were counted except those at the “look-up” level (2 μm) and such crossing or touching the forbidden planes. Four sections spaced 250 μm apart were evaluated bilaterally per animal and staining for the striatum. For the cerebellum, two cortical fields extending for approximately 600 μm on both side of the sagittal line were analyzed in each of 4 spaced-serial sections selected per animal and staining.

3.4.4 Estimation of volume of striatum and layer thickness in the cerebellum

The volume of a defined segment of the striatum (see above definition for selection of section for analysis) was estimated according to the method of Cavalieri (Howard and Reed 1998). The outlines of the striatal boundaries

required for estimation of cell densities (see above) were used to determine areas of the structure in coronal sections with the Neurolucida software. The volume was calculated in mm^3 by multiplying the sum of the areas per section (left and right side averaged for each section) by the distance between sections, i.e. 250 μm . To estimate the average thickness of the molecular and granular cell layers of the cerebellum, we divided the area of each delineated field used for estimation of cell densities by the length of its boundary facing the meningeal surface (Irintchev et al. 2005).

3.4.5 Photographic documentation

Photographic documentation was made on an Axiophot 2 microscope equipped with a digital camera AxioCam HRC and Axio Vision Software (Zeiss) at highest resolution (2300 x 2030pixel, RGB). The images were processed with AdobePhotoshop 6.0 software (Adobe System Inc., San Jose, California, USA).

3.4.6 Statistical analysis

Analysis of variance (ANOVA) with subsequent Turkey *post hoc* tests was used to compare group mean values. Analyses were performed using the SYSTAT 9 software package (SPSS, Chicago, IL, USA). By two or more measurements per parameter and animal, the mean was used as a representative value. Thus, for all comparisons the degree of freedom was determined by the number of animals. The threshold value for acceptance of differences between groups was 5%. Sigma Plot 8 software (SPSS) was used for regression analyses.

4 RESULTS

4.1 Immunohistochemical markers, quality of staining and qualitative observations in TN-R^{+/+} and TN-R^{-/-} animals

For a given staining, all sections were stained in the same primary and secondary antibody solutions. The solutions were kept in staining jars and stabilized in order to allow repeated long-term usage for a particular antigen (Irintchev et al. 2005). As formerly documented, the reproducibility of this staining technique was also apparent in this study: quality of staining remained constant for all sections processed over a period of several months. This is an important prerequisite for quantitative studies on a large number of animals. No qualitative differences between TN-R^{+/+} and TN-R^{-/-} animals were noticed in the staining patterns for the detected antigens.

The antibodies used in this study recognize specific cell-marker antigens known to be expressed in defined cell populations (Irintchev et al. 2005):

- **NeuN** (neuron-specific nuclear antigen) is a protein of unknown function shown to be present in all neurons in the adult brain with the exception of a few cell types (Purkinje, mitral and photoreceptor cells, Wolf et al. 1996)
- **PV** (parvalbumin) is a low molecular weight calcium-binding protein expressed in a major subpopulation of the GABAergic neurons
- **ChAT** (choline acetyltransferase) is a specific marker for cholinergic interneurons in the striatum
- **S-100** is a low molecular weight calcium-binding protein expressed in astrocytes

- **CNPase** (2',3'-cyclic nucleotide 3'-phosphodiesterase) is an enzyme present only in cells which are able to synthesize myelin, i.e. oligodendrocytes and Schwann cells

- **Iba1** is a macrophage/microglia-specific calcium-binding protein involved in the activation of quiescent microglial cells (Imai and Kohsaka 2002).

Examples of different stainings are shown in Fig. 2.

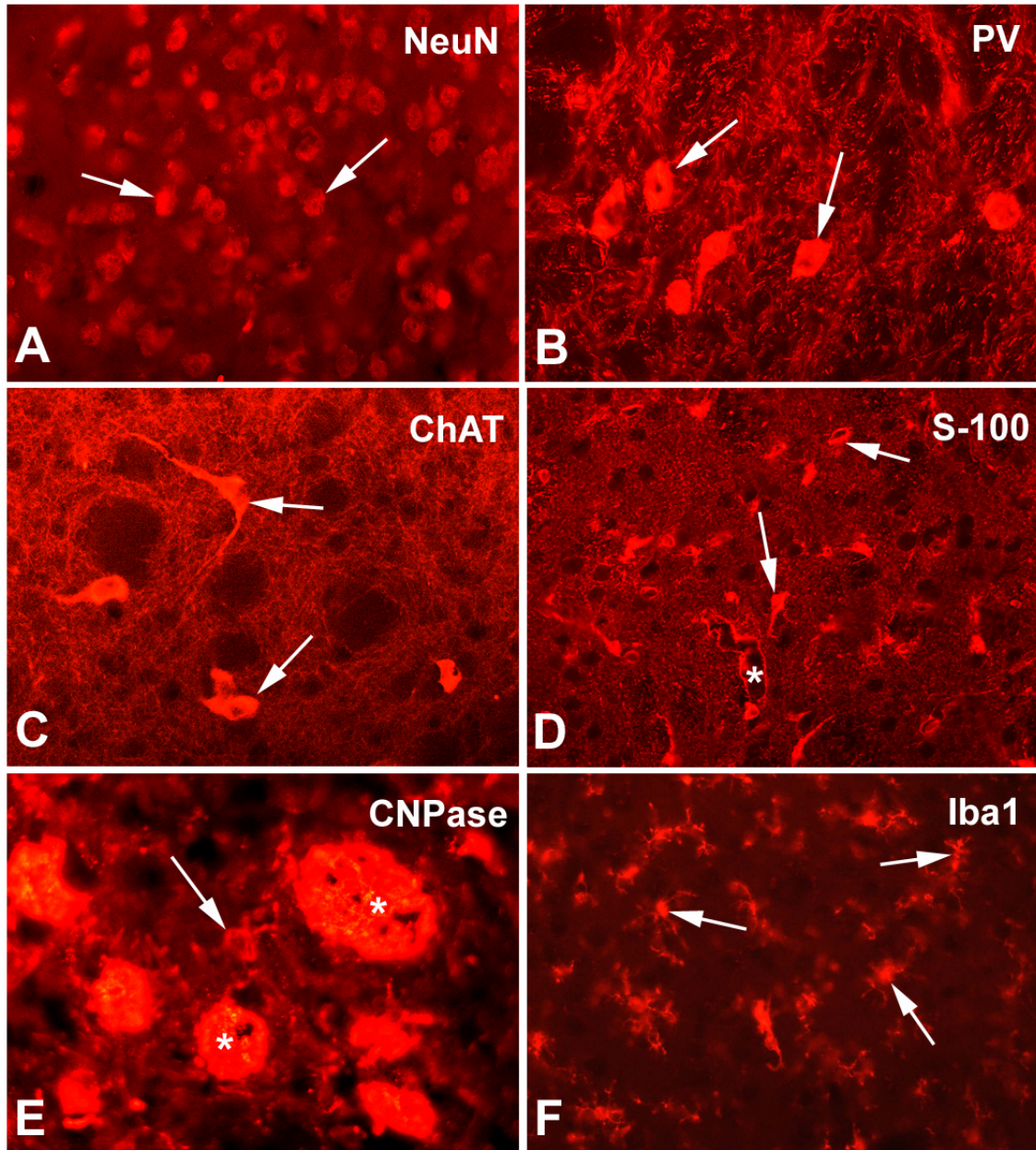


Figure 2: Examples of the immunohistochemical stainings used for quantitative analyses. Coronal brain sections from the striatum of adult (A,B,D,E) and old (C,F) TN-R deficient (A,C,D) and wild-type littermates (B,E,F). Arrows point to individual cell profiles. Note perivascular staining for S-100 and staining of myelinated axonal bundles for CNPase (asterisks in D and E, respectively).

4.2 Stereological Analyses of the Striatum

4.2.1 Volume of the Striatum

The volume of a defined segment of the striatum was determined using the Cavalieri method (see above). The volume of the striatum in 5-month-old TN-R^{-/-} animals did not differ from that of the 5-month-old TN-R^{+/+} animals (Fig. 3). Similar results were obtained for 18-month-old animals. There were also no differences between 5-month-old and 18-month-old animals.

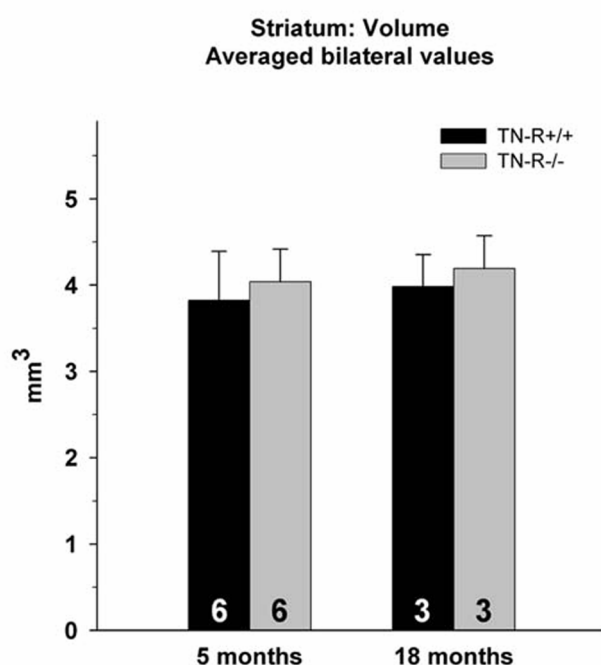


Figure 3: Volume of a defined segment of the striatum of TN-R^{+/+} (black bars) and TN-R^{-/-} (grey bars) animals studied at the age of 5 months and 18 months. Shown are averaged bilateral values + SD. Numbers of animals studied per group are indicated at the base of each bar. No significant differences were detected (ANOVA).

4.2.2 Total cell density

The nuclear staining was used to estimate the numerical density (i.e., number per unit volume) of all cells as a reference value indicative of global alterations in the striatum. The results showed no differences between TN-R^{-/-} animals and TN-R^{+/+} animals at the age of 5 month as well as at the age of 18

month (Fig. 4). There were also no differences between 5-month-old and 18-month-old animals. Since volume of the striatum was similar in all groups (see 4.2.1), cell densities of all cells, as well as of all other cell types described below, reflect total number of cells.

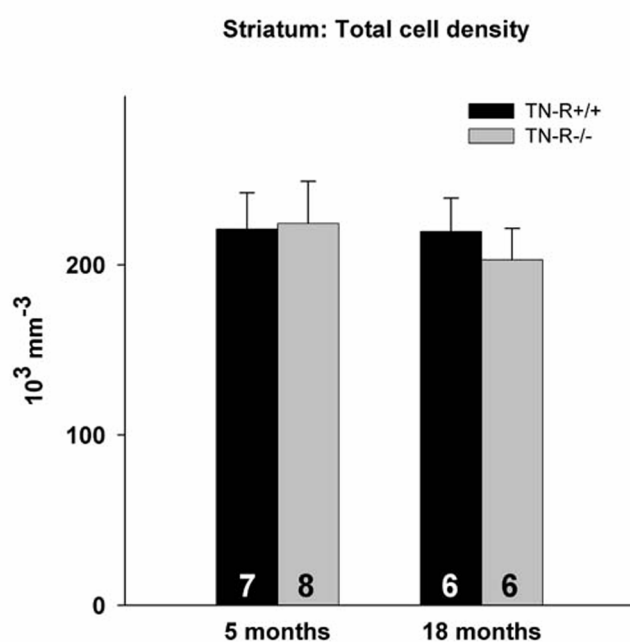


Figure 4: Total cell density in the striatum of TN-R+/+ (black bars) and TN-R-/- (grey bars) animals studied at the age of 5 months and 18 months. Shown are mean values + SD. Numbers of animals studied per group are indicated at the base of each bar. No significant differences were found (ANOVA).

4.2.3 Total neuronal population

At the age of both 5 and 18 months TN-R-/- animals did not differ from TN-R+/+ mice (Fig. 5). A significant decrease of NeuN-positive cells in old animals from both genotypes compared to young (5-month-old) mice was found (Fig. 5).

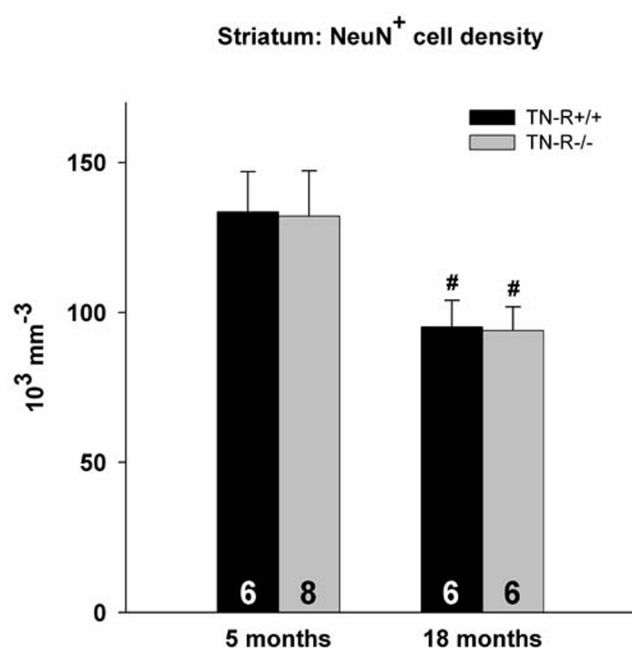


Figure 5: Total neuronal cell density in the striatum of TN-R+/+ (black bars) and TN-R-/- (grey bars) animals studied at the age of 5 months and 18 months. Shown are mean values + SD. Numbers of the mice studied per group are indicated at the base of each bar. Crosshatches indicate significant differences as compared to younger animals (ANOVA and Turkey post-hoc test).

4.2.4 Interneurons

4.2.4.1 Parvalbumin-positive interneurons

The density of PV-positive cells was similar in 5-month-old TN-R-/- and TN-R+/+ mice. In old mice, cell density was significantly higher in TN-R-/- mice compared with both wild-type littermates (+25%) and adult TN-R-/- mice (+46%)(Fig. 6). Cell density was also significantly higher in old TN-R+/+ mice compared with adult wild-type animals (+27%).

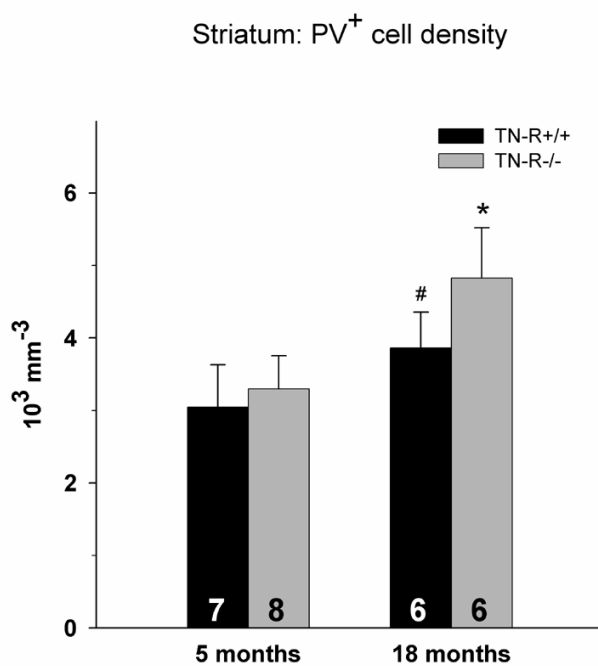


Figure 6: Density of parvalbumin-positive interneurons in the striatum of TN-R+/+ (black bars) and TN-R-/- (grey bars) animals studied at the age of 5 months and 18 months. Shown are mean values + SD. Numbers of animals studied per group are indicated at the base of each bar. Asterisk indicates significant difference as compared to both younger animals and the age-matched wild-type group, crosshatch – to the 5-month-old wild-type mice (ANOVA and Turkey post-hoc test).

4.2.4.2 Cholinergic interneurons of the striatum

The density of ChAT-positive cells was similar in all groups studied (Fig. 7).

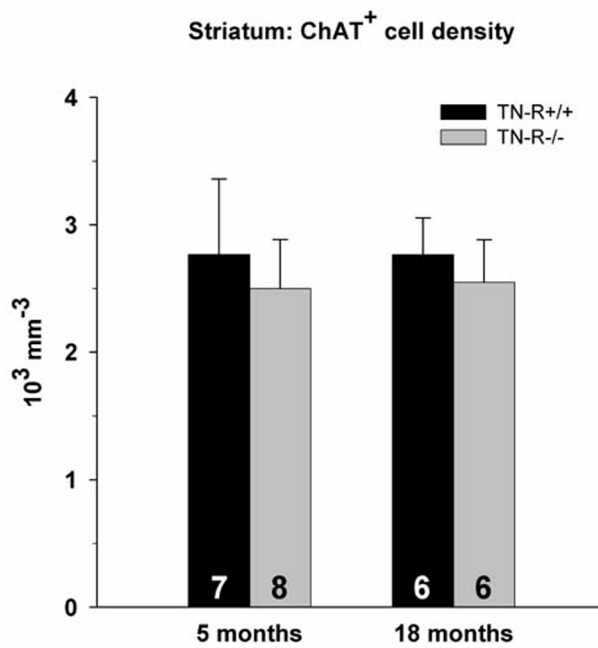


Figure 7: Density of cholinergic interneurons in the striatum of TN-R+/+ (black bars) and TN-R-/- (grey bars) animals studied at the age of 5 months and 18 months. Shown are mean values + SD. Numbers of animals studied per group are indicated at the base of each bar. No significant differences were found (ANOVA).

4.2.5 Glial cells

4.2.5.1 Oligodendrocytes

Significant age- and genotype-related differences were not observed for CNPase-positive oligodendrocytes (Fig. 8).

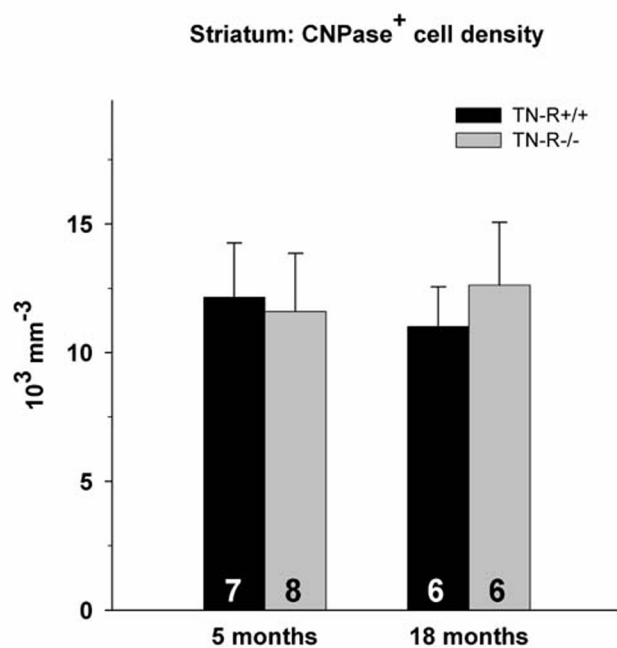


Figure 8: Densities of oligodendrocytes in the striatum of TN-R+/+ (black bars) and TN-R-/- (grey bars) animals studied at the age of 5 months and 18 months. Shown are mean values + SD. Numbers of animals studied per group are indicated at the base of each bar. No significant differences (ANOVA).

4.2.5.2 Astrocytes

At the age of 5 month, densities of S-100-positive cells in TN-R-/- and TN-R+/+ mice were similar (Fig. 9). The same was true for old animals, but, for both genotypes, a large increase was seen compared to adult mice (+36% and 50% for TN-R+/+ and TN-R-/- mice, respectively).

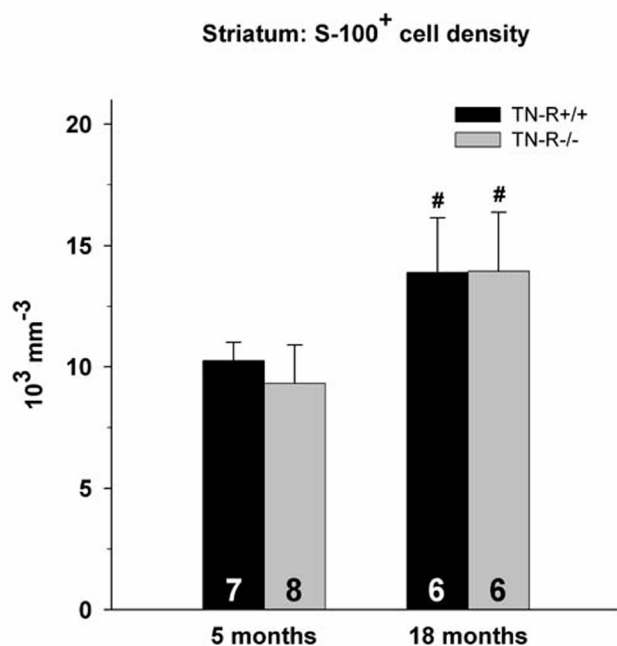


Figure 9: Densities of astrocytes of the striatum of TN-R+/+ (black bars) and TN-R-/- (grey bars) animals studied at the age of 5 months and 18 months. Shown are mean values + SD. Numbers of animals studied per group are indicated at the base of each bar. Crosshatches indicate significant differences as compared to younger animals (ANOVA and Turkey post-hoc test).

4.2.5.3 Microglia

Cell density in the TN-R-/- mice was higher (+13%) compared with TN-R+/+ mice at the age of 5 months (Fig. 10). In old animals of both genotypes densities were similar to that in adult wild-type mice.

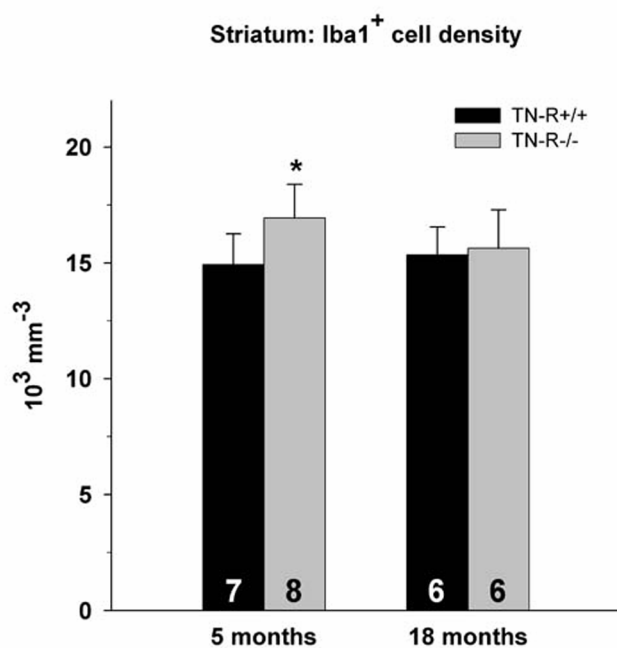


Figure 10: Densities of microglia in the striatum of TN-R+/+ (black bars) and TN-R-/- (grey bars) animals studied at the age of 5 months and 18 months. Shown are mean values + SD. Numbers of animals studied per group are indicated at the base of each bar. Asterisk indicates significant difference compared to age-matched wild-type animals (ANOVA and Turkey post-hoc test).

4.3 Stereological Analyses of the Cerebellum

4.3 1 Thickness of the molecular layer and the granular layer

The normalized thickness was calculated as ratio of the layer segment area to the length of the surface (meningeal) boundary of the segment. Layer thickness was similar in the two genotype groups at both ages studied, in the molecular layer (Fig. 11) as well as in the granular layer (Fig. 12). This finding is important with regard to the interpretation of differences in cell densities in terms that, as for the striatum, cell densities reflect absolute cell numbers.

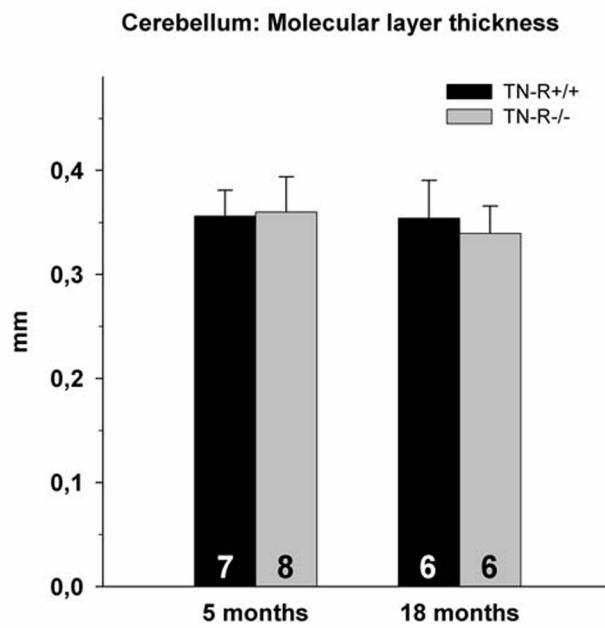


Figure 11: Thickness of the molecular layer in the cerebellum of TN-R+/+ (black bars) and TN-R-/- (grey bars) animals studied at the age of 5 months and 18 months. Shown are mean values + SD. Numbers of animals studied per group are indicated at the base of each bar. No significant differences were found (ANOVA).

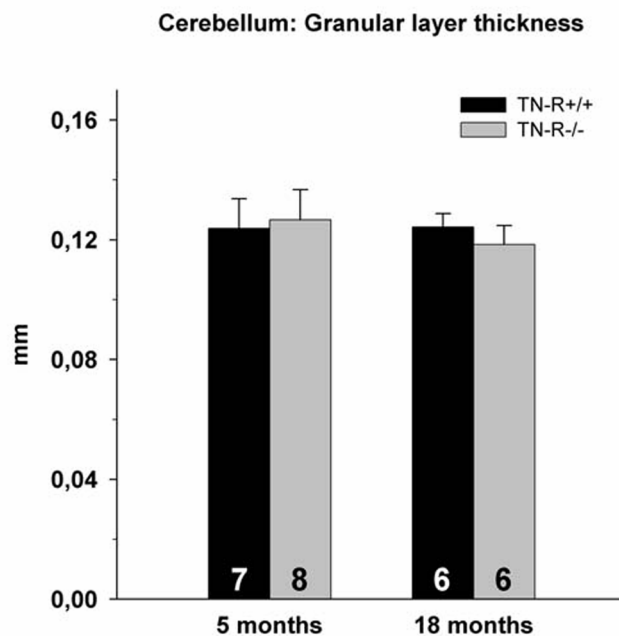


Figure 12: Thickness of the granular layer in the cerebellum of TN-R+/+ (black bars) and TN-R-/- (grey bars) animals studied at the age of 5 months and 18 months. Shown are mean values + SD. Numbers of the animals studied per group are indicated at the base of each bar. No significant differences were found (ANOVA).

4.3.2 Total neuronal population of the granular layer

The total neuronal population in the granular layer (NeuN⁺ staining) of TN-R^{-/-} animals did not differ from the TN-R^{+/+} animals at the age of 5 months as well as at the age of 18 months (Fig. 13). There were also no age-related differences.

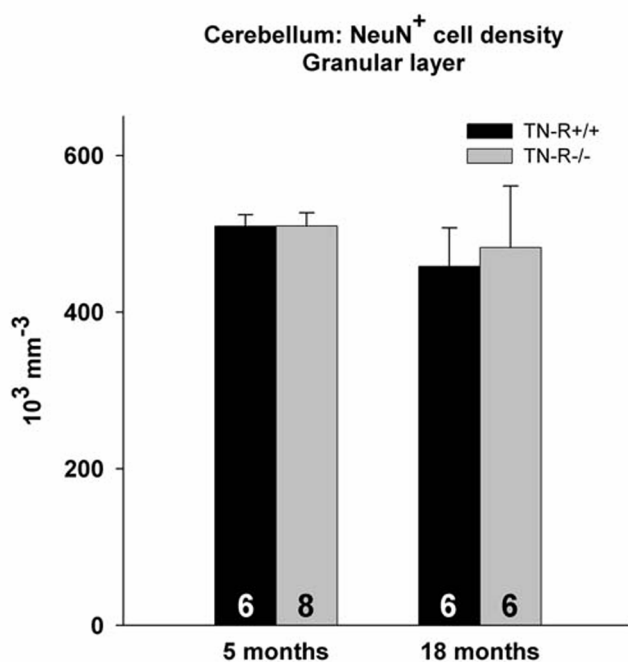


Figure 13: Total neuronal population in the granular layer of the cerebellum of TN-R^{+/+} (black bars) and TN-R^{-/-} (grey bars) animals studied at the age of 5 months and 18 months. Shown are mean values + SD. Numbers of animals studied per group are indicated at the base of each bar. No significant differences were found (ANOVA).

4.3.3 Interneurons

4.3.3.1 Parvalbumin-positive interneurons (basket, stellate and Golgi cells)

Density of parvalbumin-positive interneurons was significantly higher in both adult and old TN-R deficient mice compared with wild-type littermates (+49% and +31%, respectively) (Fig. 14). Age-related differences within the genotypes were not found.

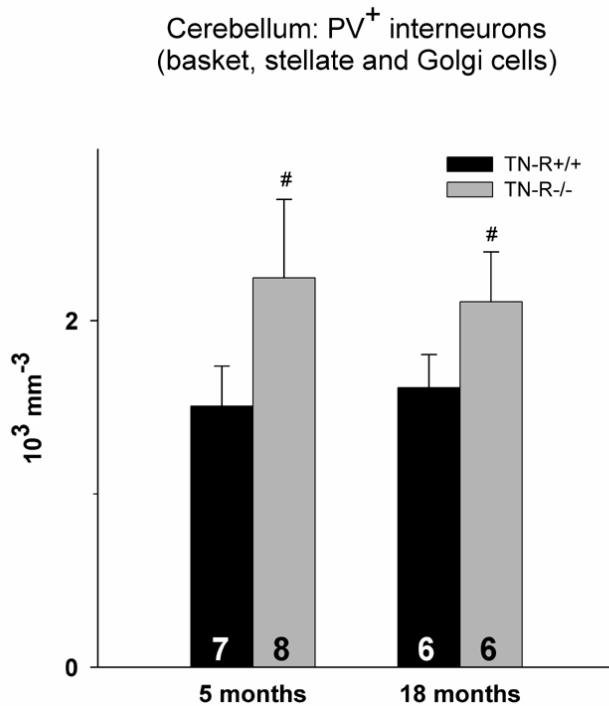


Figure 14: Densities of parvalbumin-positive interneurons in the cerebellum of TN-R+/+ (black bars) and TN-R-/- (grey bars) animals studied at the age of 5 months and 18 months. Shown are mean values + SD. Numbers of animals studied per group are indicated at the base of each bar. Crosshatches indicate significant differences as compared to age-matched TN-R+/+ animals (ANOVA and Turkey post-hoc test).

4.3.3.2 Purkinje neurons

Densities of Purkinje neurons, identified by their size, position and positive staining for parvalbumin, were similar in all groups studied (Fig. 15).

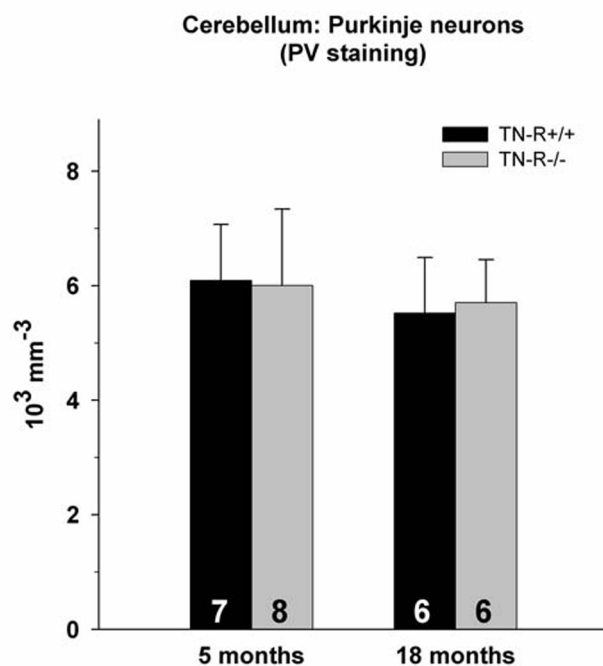


Figure 15: Densities of Purkinje neurons in the cerebellum of TN-R+/+ (black bars) and TN-R-/- (grey bars) animals studied at the age of 5 months and 18 months. Shown are mean values + SD. Numbers of animals studied per group are indicated at the base of each bar. No significant differences were found (ANOVA).

4.3.3.3 Ratio Purkinje cells / interneurons (basket, stellate and Golgi cells)

Estimation of numerical densities of different cell types in sections from one specimen allows calculation of physiologically meaningful ratios between cell types (Irintchev et al. 2005). The ratio Purkinje cells to interneurons was significantly smaller (-33 %) in the mutant animals than in wild-type mice at the age of 5 months (Fig.16). The ratios in the older groups did not differ statistically.

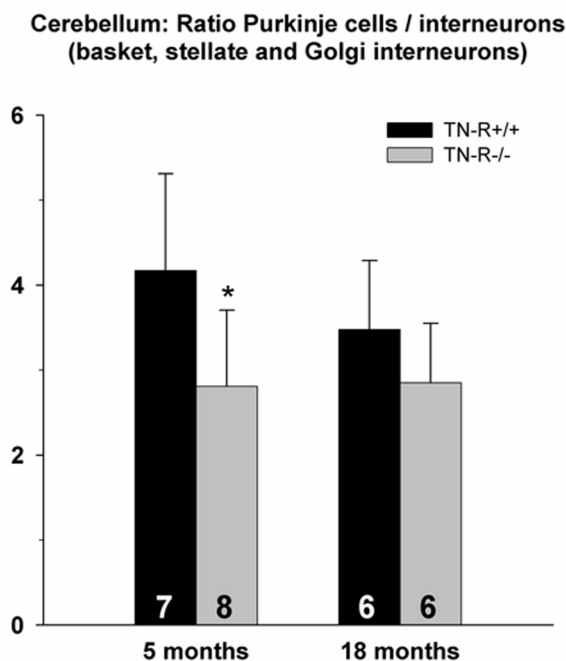


Figure 16: Ratios Purkinje cells / interneurons in the cerebellum of TN-R+/+ (black bars) and TN-R-/- (grey bars) animals studied at the age of 5 months and 18 months. Shown are mean values + SD. Numbers of animals studied per group are indicated at the base of each bar. Asterisk indicates significant difference as compared to the age-matched group (ANOVA and Turkey post-hoc test).

4.3.4 Glial cells

4.3.4.1 Oligodendrocytes in the granular layer

The number of CNPase-positive cells in 5-month-old TN-R-/- animals did not differ from that in wild-type control animals (Fig. 17). In 18-month-old mice, however, a large (+26 %) and significant increase in the density of CNPase-positive cells was found in TN-R deficient animals compared with wild-type littermates. Also in comparison with young animals, a large (+28%) and significant increase was found.

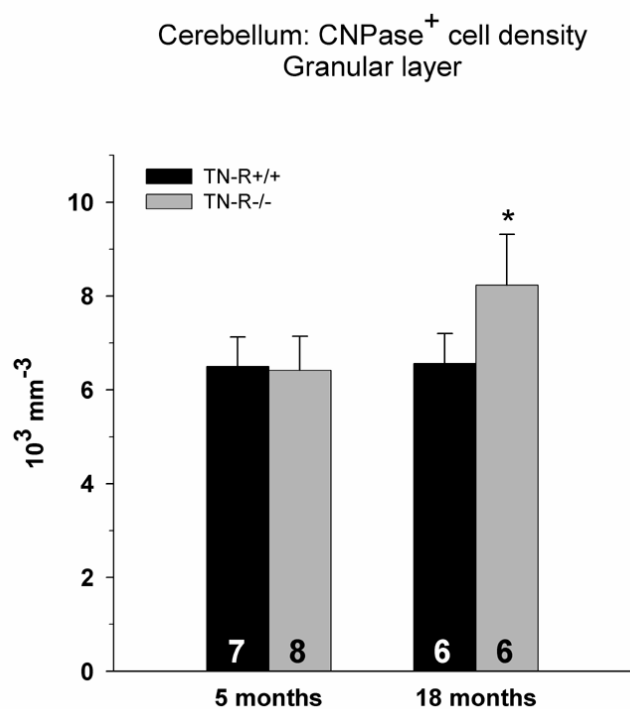


Figure 17: Densities of oligodendrocytes in the cerebellum of TN-R+/+ (black bars) and TN-R-/- (grey bars) animals studied at the age of 5 months and 18 months. Shown are mean values + SD. Numbers of animals studied per group are indicated at the base of each bar. Asterisks indicate significant differences as compared to all other groups (ANOVA and Turkey post-hoc test).

4.3.4.2 Astrocytes in the cerebellum

At 5 months of age density of S-100-positive cells did not differ between TN-R-/- and TN-R+/+ mice. A significant increase in density, as compared with adult animals, was found in old TN-R+/+ mice (+ 20%) but not in TN-R-/- animals (+14%, not significant) (Fig.18).

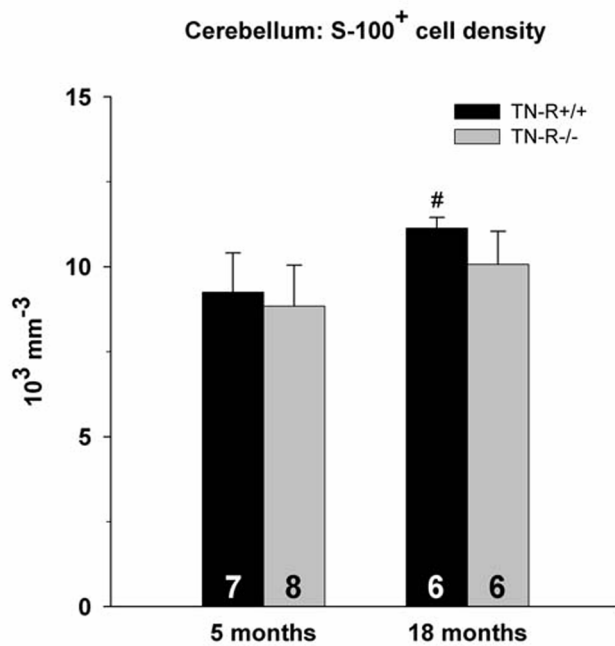


Figure 18: Densities of astrocytes in the cerebellum of TN-R+/+ (black bars) and TN-R-/- (grey bars) animals studied at the age of 5 months and 18 months. Shown are mean values + SD. Numbers of animals studied per group are indicated at the base of each bar. Crosshatch indicates significant difference as compared to the younger animals (ANOVA and Turkey post-hoc test).

4.3.4.3 Microglia

Densities of microglial cells were similar in all groups studied (Fig. 19).

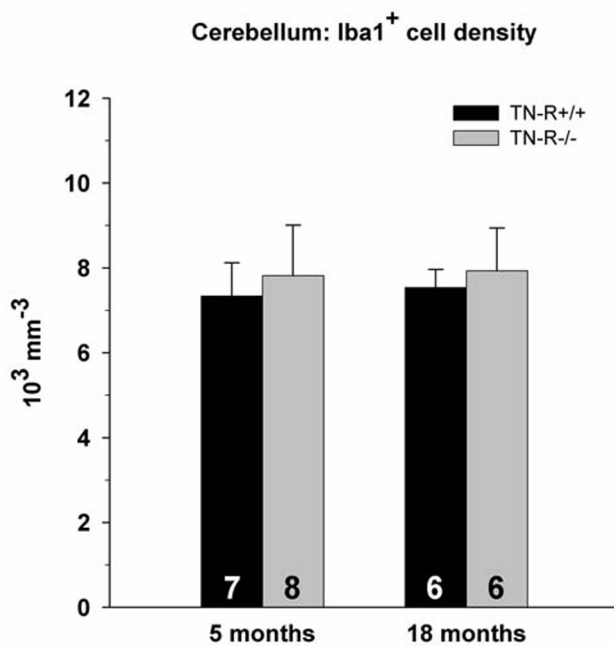


Figure 19: Densities of microglia in the cerebellum of TN-R+/+ (black bars) and TN-R-/- (grey bars) animals studied at the age of 5 months and 18 months. Shown are mean values + SD. Numbers of animals studied per group are indicated at the base of each bar. No significant differences were found (ANOVA).

5 DISCUSSION

This study provided quantitative data on the size of major cell populations in the cerebellum and striatum of both adult (5-month-old) and old (18-20-month-old) TN-R deficient mice and wild-type littermates. The results, summarized in Table 1, show both genotype-specific and age-related changes in neuronal and glial subpopulations thus providing novel insights into the importance of TN-R for the formation and structural maintenance of the striatum and cerebellum as well as into the impacts of aging on these two brain areas in the genetically normal laboratory mouse.

Table 1. Summary of age- and phenotype-related differences

Parameter / Cell type	Genotype-related differences TN-R ^{-/-} versus TN-R ^{+/+}		Age-related differences 18 months versus 5 months	
	5 months	18 months	TN-R ^{+/+}	TN-R ^{-/-}
	Striatum			
Volume	=	=	=	=
All cells	=	=	=	=
All neurons	=	=	↓ (-29%)	↓ (-29%)
PV+ neurons	=	↑ (+25%)	↑ (+27%)	↑ (+46%)
ChAT+ neurons	=	=	=	=
Oligodendrocytes	=	=	=	=
Astrocytes	=	=	↑ (+36%)	↑ (+50%)
Microglia	↑ (+13%)	=	=	=

Cerebellum				
Thickness, mol. l.	=	=	=	=
Thickness, gran. l.	=	=	=	=
Granule cells	=	=	=	=
PV+ neurons	↑ (+49%)	↑ (+31%)	=	=
Purkinje cells	=	=	=	=
Oligodendrocytes	=	↑ (+26%)	=	↑ (+28%)
Astrocytes	=	=	↑ (+20%)	=
Microglia	=	=	=	=

Statistically significant (↑,↓) and non-significant (=) differences (ANOVA and post hoc Turkey test) between group mean values. Numbers in brackets indicate the difference in percent between the two mean values. PV – parvalbumin; ChAT – choline acetyltransferase, mol. l. – molecular layer; gran. l. – granular layer..

5.1 Genotype-related aberrations in adult mice

TN-R is first detectable in the mouse brain around birth and its peak expression is associated with the process of myelination in the central nervous system (CNS)(Bartsch et al. 1993; Wintergerst et al. 1993). After myelination has ceased, TN-R levels are down-regulated to lower levels in the adult. The protein is expressed by oligodendrocyte progenitors and oligodendrocytes. It is detectable at contact sites between unmyelinated axons, between axons and glial cells, and between axons and processes of myelinating oligodendrocytes and is accumulated at the nodes of Ranvier (Bartsch et al. 1993). TN-R is also expressed by subsets of CNS neurons, such as interneurons in the cerebellum, hippocampus, spinal cord and retina, as well as motoneurons in the spinal cord (Fuss et al. 1993; Wintergerst et al. 1993; Weber et al. 1999). It is localized in perineuronal nets that surround these neurons (Adams et al. 2001; Bruckner et

al. 2000; Wintergerst et al. 1996). In contrast to oligodendrocytes, the expression of TN-R by neurons is not down-regulated in the adulthood (Fuss et al. 1993).

Previous studies have shown that the general histological appearance of major brain structures in TN-R deficient mice is normal (Weber et al. 1999). Qualitative analyses of TN R^{-/-} mice have indicated that the molecular layer, the Purkinje cell layer and the internal granular layer of the cerebellum as well as the inner and outer nuclear layer and the plexiform layers of the retina are normally developed. No structural aberrations in the spinal cord of TN-R^{-/-} mice have been detected, either (Weber et al. 1999). In agreement with these observations, the results of the quantitative analyses of the cerebellum and the striatum showed that the size of these brain structures, as evaluated by estimation of the striatal volume and thickness of cerebellar cortex layers, in adult (5-months-old) TN-R deficient mice was similar to those in wild-type littermates (Table 1). Also, densities of all cell types, with the exception of microglial cells in the striatum and parvalbumin-positive cells in the cerebellum, were normal in the adult TN-R deficient mice (Table 1). It is important to note that cell densities reflect total numbers of cells to the same degree for TN-R^{-/-} and TN-R^{+/+} mice since no differences in size of the analysed structures were observed.

The reasons for the increase in the number of microglial cells in the striatum of 5- but not 18-month-old TN-R^{-/-} mice compared to wild-type littermates (Table 1) are not readily explainable. Microgliosis is usually associated with brain tissue destruction as a result of, for example, traumata, degenerative, inflammatory or autoimmune diseases. The previous

observations of normal brain morphology and the current findings of normally sized cell populations in the striatum of adult TN-R deficient mice allows the conclusion that abnormal numbers of microglial cells in the knockout mice are not due to tissue degeneration. The phenomenon cannot also be associated with age-related loss of neurons since such loss similarly affected both genotypes (see below) and should proceed gradually at a slow rate. The reasons for the modest increase in number of microglial cells in adult TN-R^{-/-} mice cannot be, therefore, readily explained.

In contrast to microglial cells, PV⁺ interneurons in the cerebellum synthesize TN-R in the adult rodent brain (Carulli et al. 2006; Fuss et al. 1993). Therefore, the abnormally high numbers of these cells in adult TN-R^{-/-} mice (+49% compared to wild-type littermates) can be directly attributed to the absence of TN-R which accumulates in the perineuronal nets surrounding these interneurons. PV⁺ interneurons, including stellate, basket and Golgi cells, are formed by dividing precursor cells in the white matter and migrate to the outer molecular layer (basket and stellate cells) and the inner granular layer (Golgi cells) during the first two postnatal weeks (Sotelo 2004). During this developmental time-period, TN-R mRNA expression is detectable starting at postnatal day 0 (P0) in the white matter and at P7 in the outer molecular layer (Fuss et al. 1993). Therefore, initiation of TN-R expression in the cerebellum coincides spatially and temporally with the formation of the PV⁺ interneurons in the cerebellum and could influence the proliferation or the naturally occurring cell death in the postnatal period. In contrast to the cerebellum, the numbers of PV⁺ cells in the striatum of adult TN-R^{-/-} mice were normal (Table 1). Previous observations have suggested that the populations of PV⁺ interneurons in the

somatosensory cortex, retrosplenial cortex and the hippocampus are also normal (Brenneke et al. 2004; Saghatelian et al. 2001; Weber et al. 1999). Although in all above-mentioned brain areas the PV⁺ neurons possess perineuronal nets and thus synthesize TN-R in the adulthood (Adams 2001; Bruckner et al. 2000, 2003, 2006; Murakami 2003), their number is increased in the cerebellum only. This region-specific difference of the TN-R ablation may be attributed to the early postnatal expression of the glycoprotein in the cerebellum (Fuss et al. 1993) as opposed to other brain regions such as the hippocampus where TN-R is barely detectable before the third postnatal week (Bruckner et al. 2000). From these considerations it can be concluded that the present results provide evidence for an essential developmental role of TN-R in shaping the size of major subpopulations of interneurons in the cerebellum.

5.2 Genotype-related aberrations in old mice

In addition to adult mice, old TN-R^{-/-} mice and wild-type littermates were included in this study in order to test the hypothesis that compensatory mechanisms limiting the impact of the constitutive TN-R ablation during adulthood may become deficient with aging. The analysis revealed that, indeed, in addition to persisting abnormal numbers of PV⁺ cells in the cerebellum, old (18-20 month of age) TN-R^{-/-} mice have also higher numbers of PV⁺ interneurons in the striatum (+25%) as well as of oligodendrocytes in the cerebellum (+26%) compared to wild-type littermates (Table 1). For PV⁺ cells, an increase in cell numbers between 5 and 18 months of age was found in the striatum of both TN-R^{-/-} and TN-R^{+/+} mice. This increase was much more

prominent in old TN-R^{-/-} than in TN-R^{+/+} mice (+46% and +27% compared to adult wild-type littermates, respectively). A straightforward explanation of these observations is that during normal aging PV-negative GABAergic interneurons (somatostatin- or calretinin-positive, Tepper and Bolam 2004) in the striatum change their expression profile and become PV-positive and that this process is enhanced by TN-R deficiency. Novel findings that new striatal interneurons are generated in both the intact and post-ischemic adult rodent brain (Dayer et al. 2005; Teramoto et al. 2003) allow to speculate that increased numbers of PV⁺ cells may result from age-related alterations in the neuronogenesis. Numbers of CNPase-positive oligodendrocytes were similar in old TN-R^{+/+} mice and adult mice of both genotypes (Table 1). Therefore, the abnormally high numbers of oligodendrocytes in the cerebellum of old TN-R^{-/-} mice (+26% compared to wild-type littermates) is due to proliferation and thus enlargement of the population size. Similar age-related alteration was not observed in the striatum (Table 1). The increase in oligodendrocyte numbers in the old TN-R^{-/-} cerebellum may be interpreted as a reaction aiming to compensate deficient cell functions becoming more prominent with age. It is important to stress that all cell types found to be affected in adult and old TN-R^{-/-} mice normally express TN-R which indicates specific direct consequences of the TN-R ablation rather than secondary phenomena.

5.3 Age-related changes

Apart of age-related changes in the PV⁺ interneurons in both genotypes (see above), the results of this study show that aging leads to genotype-

independent increase in the number of astrocytes in the cerebellum and striatum and loss of NeuN⁺ neurons in the striatum of wild-type mice (Table 1). The astrogliosis in the striatum was pronounced in both TN-R^{+/+} and TN-R^{-/-} old mice (36% and 50% increase of the S-100-positive cells in both groups compared to wild-type littermates, respectively). The age-related increase in astrocytes in the cerebellum was modest in wild-type mice (+20%) and less so in TN-R^{-/-} mice (+14%, not significant). These findings are consistent with previous results of stereological analyses of astrocytes in the aged mouse hippocampus (Lei et al. 2003; Mouton et al. 2002). Lei et al. 2003 and Mouton et al. 2002 report also an age-related increase in the number of microglial cell in the hippocampus which was not observed in this study. This discrepancy may be due to brain region-specific differences in the aging processes or to use of different microglia markers, Mac-1 in the previous studies versus Iba1 used here.

Precise stereological estimates of neuronal numbers in the neocortex, cerebellar cortex and hippocampus of rodents, primates and humans in the recent years have shown that normal neuronal numbers are maintained in aged subjects, findings fundamentally changing the widely accepted old view that age-related impairment of brain functions result from neuronal loss (Andersen et al. 2003; Hof and Morrison 2004; Long et al. 1999; Morrison and Hof 1997). In agreement with these findings are the observations of preserved neuronal numbers in the cerebellum of old mice analysed in this study (Table 1). In the striatum, however, numbers of NeuN⁺ neurons in both TN-R^{-/-} and TN-R^{+/+} old mice were reduced by 29% as compared to adult animals (Table 1). It cannot be excluded that the observed age-related difference results from loss of NeuN

expression in a significant proportion of the striatal neurons. If this were the case, this change in the expression profile of the striatal neurons is in contrast to the cerebellar granule cells, similar in numbers in old and adult mice, though also analysed using NeuN⁺ immunohistochemistry. Another possibility is that changes in NeuN⁺ cell numbers reflect real loss of neurons. Such loss of neurons will be restricted to medium spiny projection neurons since they comprise 90 - 97% of the neuronal cells in the rodent striatum (Zhou et al. 2002; Tepper and Bolam 2004). A profound deficit in the projecting neurons would inevitably have significant impacts on motor and cognitive functions in which the neostriatum is implicated (Packard and Knowlton 2002).

5.4 Possible functional significance of the structural aberrations in TN-R deficient mice

Behavioural analyses have revealed that adult TN-R deficient mice have motor deficits under demanding conditions but the underlying structural abnormalities have not been identified (Freitag et al. 2003). The finding that major cell populations in the striatum are normal in size in adult TN-R^{-/-} mice indicates that structural aberrations in this brain area do not underlie the observed motor deficits. In the cerebellum of knockout mice, the number of PV⁺ interneurons was found to be increased by 49% and the ratio Purkinje cells / PV interneurons by -33%. Such profound structural abnormalities must have functional consequences. Therefore, it can be concluded that this study provides evidence that impaired motor behaviour of TN-R deficient mice results, at least in part, from aberrations in the structure of the cerebellum.

6 SUMMARY

Tenascin-R (TN-R) is a glycoprotein of the tenascin family of extracellular matrix proteins. It is expressed in the CNS by oligodendrocytes, horizontal cells in the retina, Purkinje, stellate and basket cells in the cerebellum, motoneurons in the spinal cord and interneurons in the hippocampus. TN-R is an essential component of the perineuronal nets around motoneurons and interneurons and has been implicated in cell adhesion, neurite outgrowth, modulation of ion channel and receptor functions, synaptic plasticity and learning.

TN-R deficient mice have a range of behavioural and physiological abnormalities and impaired motor coordination. Previous studies have failed to detect structural abnormalities in the knockout (ko) mouse with a few exceptions: disorganization of perineuronal nets, decreased number of calretinin-positive cells in the hippocampus and reduced coverage of pyramidal neuronal cell bodies in the CA1 region of the hippocampus by inhibitory synapses.

This study was designed to further characterize the TN-R deficient mouse with respect to morphological abnormalities in the brain structures known to be involved in motor control. Performed were morphometric analyses and stereological estimations of immunohistochemically identified major cell types (neurons, neuronal subpopulations, astrocytes, oligodendrocytes and microglia). The areas analysed included the neostriatum (nucleus caudatus and putamen) and the cerebellum. Both TN-R-deficient mice (TN-R^{-/-}) and wild-type (TN-R^{+/+}) littermates were studied at ages of 5 and 18 months, i.e. adult and old age, respectively.

The results showed that adult TN-R deficient mice have normal numbers of neurons, parvalbumin interneurons, cholinergic interneurons, oligodendrocytes and astrocytes, as well as normal striatal volume. A slight increase in the number of microglial cells (+13%) was found. In old TN-R^{-/-} mice, all cell populations studied, including microglia, were normal in size with the exception of parvalbumin interneurons which were more numerous than in wild-type littermates (+25%). Comparisons of old and adult mice showed a genotype-unrelated increase in astrocyte numbers (+36%) and loss of NeuN-positive neurons (-29%) with age. An age-related increase in the number of parvalbumin interneurons was also observed in wild-type mice (+27%) but this was less pronounced than in TN-R^{-/-} mice (+46%).

In the cerebellum of adult TN-R^{-/-} mice, a marked increase in the number of parvalbumin interneurons (stellate, basket and Golgi cells) was found (+49% compared to TN-R^{+/+} littermates). Numbers of Purkinje and granule cells, as well as astrocytes, oligodendrocytes and microglia were normal in adult TN-R^{-/-} mice. The abnormally high numbers of parvalbumin interneurons was preserved in old TN-R^{-/-} mice. In addition, an age-related increase in the number of oligodendrocytes (+26%) was found in TN-R^{-/-} mice but not in wild-type animals. Similar to the striatum, astrocyte numbers increased in the cerebellum with aging independent of genotype.

The results of this study show that deficient expression of TN-R leads to the formation of an abnormally large populations of interneurons in the cerebellum. This finding suggests a novel role TN-R in regulating the size of cell populations that normally expressed it during their formation. Alterations in the numbers of oligodendrocytes in the cerebellum and parvalbumin neurons in the

striatum of old TN-R^{-/-} mice, cell types that normally express TN-R during adulthood, can be interpreted as signs of age-related insufficiency of compensatory mechanisms counteracting the consequences of TN-R deficiency. The motor deficits previously observed in TN-R deficient mice may be related to the abnormal interneuron populations in the cerebellum.

7 REFERENCES

Adams I, Brauer K, Arelin C, Hartig W, Fine A, Mader M, Arendt T, Bruckner G (2001) Perineuronal nets in the rhesus monkey and human basal forebrain including basal ganglia. *Neuroscience* 108: 285-298.

Andersen BB, Gundersen HJ, Pakkenberg B (2003) Aging of the human cerebellum: a stereological study. *J Comp Neurol* 466: 356-365.

Angelov DN, Walther M, Streppel M, Guntinas-Lichius O, Neiss WF, Probstmeier R, Pesheva P (1998) Tenascin-R is antiadhesive for activated microglia that induce downregulation of the protein after peripheral nerve injury: a new role in neuronal protection. *J Neurosci* 18(16): 6218-6229.

Bartsch U, Pesheva P, Raff M, Schachner M (1993) Expression of janusin (J1-160/180) in the retina and optic nerve of the developing and adult mouse. *Glia* 9: 57-69.

Bartsch S, Bartsch U, Dörries U, Faissner A, Weller A, Ekblom P, Schachner M (1992b) Expression of Tenascin in the developing and adult cerebellar cortex. *J Neurosci* 12(3): 736-749.

Becker T, Anliker B, Becker CG, Taylor J, Schachner M, Meyer RL, Bartsch U (2000) Tenascin-R inhibits regrowth of optic fibers in vitro and persists in the optic nerve of mice after injury. *Glia*, 29: 330-346.

Becker CG, Schweitzer J, Feldner J, Becker T, Schachner M (2003) Tenascin-R as a repellent guidance molecule for developing optic axons in zebrafish. *J Neurosci* 23(15): 6232-6237.

Brenneke F, Bukalo O, Dityatev A, Lie AA (2004) Mice deficient for the extracellular matrix glycoprotein tenascin-R show physiological and structural hallmarks of increased hippocampal excitability, but no increased susceptibility to seizures in the pilocarpine model of Epilepsy. *Neuroscience* 124: 841-855.

Bruckner G, Grosche J, Schmidt S, Hartig W, Margolis RU, Delpech B, Seidenbecher CI, Czaniera R, Schachner M (2000) Postnatal development of perineuronal nets in wild-type mice and in a mutant deficient in tenascin-R. *J Comp Neurol* 428: 616-629.

Bruckner G, Grosche J, Hartlage-Rubsamen M, Schmidt S, Schachner M (2003) Region and lamina-specific distribution of extracellular matrix proteoglycans, hyaluronan and tenascin-R in the mouse hippocampal formation. *J Chem Neuroanat* 26: 37-50.

Bruckner G, Szeoke S, Pavlica S, Grosche J, Kacza J (2006) Axon initial segment ensheathed by extracellular matrix in perineuronal nets. *Neuroscience* 138: 365-375.

- Bukalo O, Schachner M, Dityatev A (2001) Modification of extracellular matrix by enzymatic removal of chondroitin sulphate and by lack of tenascin-R differentially affects several forms of synaptic plasticity in the hippocampus. *Neuroscience*, 104(2): 359-369.
- Carnemolla B, Leprini A, Borsi L, Querze G, Urbini S, Zardi L (1996) Human tenascin-R (Complete primary structure, PRE-mRNA, alternative splicing and gene localization on Chromosome1q23-q24). *J Biol Chem* 271(14): 8157-8160.
- Carulli D, Rhodes KE, Brown DJ, Bonnert TP, Pollack SJ, Oliver K, Strata P, Fawcett JW (2006) Composition of perineuronal nets in the adult rat cerebellum and the cellular origin of their components. *J Comp Neurol* 494: 559-577.
- Celio MR, Chiquet-Ehrismann R (1993) Perineuronal nets` around cortical interneurons expressing parvalbumin are rich in tenascin. *Neurosci Lett* 162: 137-140.
- Celio MR and Blümcke I (1994) Perineuronal nets – a specialized form of extracellular matrix in the adult nervous system. *Brain Res Rev* 19: 128-145.
- Dayer AG, Cleaver KM, Abouantoun T, Cameron HA (2005) New GABAergic interneurons in the adult neocortex and striatum are generated from different precursors. *J Cell Biol* 168: 415-427.
- Erickson HP (1993) Tenascin-C, tenascin-R and tenascin-X: a family of talented proteins in search of functions. *Curr Opin Cell Biol* 5: 869-876.
- Erickson HP (1994) Evolution of the Tenascin family – implications for function of the C-terminal fibrinogen-like domain. *Perspect Dev Neurobiol* 2(1): 9-19.
- Faissner A (1997) The tenascin gene family in axon growth and guidance. *Cell Tiss Res* 290: 331-341.
- Freitag S, Schachner M, Morellini F (2003) Behavioural alterations in mice deficient for the extracellular matrix glycoprotein tenascin-R. *Behav Brain Res* 145(1-2): 189-207.
- Fuss B, Wintergerst ES, Bartsch U, Schachner M (1993) Molecular characterization and in situ mRNA localization of the neural recognition molecule J1-160/180: a modular structure similar to tenascin. *J Cell Biol* 120: 1237-1249.
- Gurevicius K, Gureviciene I, Valjakka A, Schachner M, Tanila H (2004) Enhanced cortical and hippocampal neuronal excitability in the mice deficient for the extracellular matrix glycoprotein tenascin-R. *Molecular and Cellular Neuroscience*, 25(3): 515-523.
- Gutowski NJ, Newcombe J, Cuzner ML (1999) Tenascin-R and C in multiple sclerosis lesions: a relevance to extracellular matrix remodelling. *Neuropath Appl Neurobiol* 25: 207-214.

- Hagihara K, Miura R, Kosaki R, Berglund E, Ranscht B, Yamaguchi Y (1999) Immunohistochemical evidence for the brevican-tenascin-R interaction: colocalization in perineuronal nets suggest a physiological role for the interaction in the adult rat brain. *J Comp Neurol* 410: 256-264.
- Haunso A, Ibrahim M, Bartsch U, Letiembre M, Celio MR, Menoud PA (2000) Morphology of perineuronal nets in tenascin-R and parvalbumin single and double knockout mice. *Brain Res* 864:142-145.
- Hof PR, Morrison JH (2004) The aging brain: morphomolecular senescence of cortical circuits. *Trends Neurosci* 27: 607-613.
- Howard and Reed (1998) Unbiased stereology – three dimensional measurement in microscopy. Oxford: BIOS Scientific Publications.
- Husmann K, Faissner A, Schachner M (1992) Tenascin promotes cerebellar granule cell migration and neurite outgrowth by different domains in the fibronectin type III repeats. *J Cell Biol* 116(6):1475-1486.
- Imai Y, Kohsaka S (2002) Intracellular signalling in M-CSF-induced microglia activation: Role of Iba-1. *Glia*, 40: 164-174.
- Irintchev A, Rollenhagen A, Troncoso E, Kiss JZ, Schachner M (2005) Structural and functional aberrations in the cerebral cortex of tenascin-C deficient mice. *Cereb Cortex* 15:950-962.
- Jones FS, Jones PL, (2000) The tenascin family of extracellular matrix glycoproteins: structure, function, and regulation during embryonic development and tissue remodelling. *Devel Dyn* 218:235-25
- Jung M, Pesheva P, Schachner M, Trotter J (1993) Astrocytes and Neurons regulate the expression of the neural recognition molecule Janusin by cultured Oligodendrocytes. *Glia* 9: 163-175.
- Lei DL, Long JM, Hengemihle J, O'Neill J, Manaye KF, Ingram DK, Mouton PR (2003) Effects of estrogen and raloxifene on neuroglia number and morphology in the hippocampus of aged female mice. *Neuroscience* 121: 659-666.
- Long JM, Mouton PR, Jucker M, Ingram DK (1999) What counts in brain aging? Design-based stereological analysis of cell number. *J Gerontol A Biol Sci Med Sci* 54: B407-B417.
- Montag-Sallaz M, Montag D (2003) Severe cognitive and motor coordination deficits in tenascin-R deficient mice. *Genes Brain Behav* 2: 20-31.
- Morganti MC, Taylor J, Pesheva P, Schachner M (1990) Oligodendrocyte-derived J1-160/180 extracellular matrix glycoproteins are adhesive or repulsive depending on the partner cell type and time of interaction. *Exp Neurol* 109: 98-110.

- Morrison JH, Hof PR (1997) Life and death of neurons in the aging brain. *Science* 278: 412-419.
- Mouton PR, Long JM, Lei DL, Howard V, Jucker M, Calhoun ME, Ingram DK (2002) Age and gender effects on microglia and astrocyte numbers in brains of mice. *Brain Res* 956: 30-35.
- Murakami T, Ohtsuka A (2003) Perisynaptic barrier of proteoglycans in the mature brain and spinal cord. *Arch Histol Cytol* 66: 195-207.
- Nikonenko A, Schmidt S, Skibo G, Bruckner G, Schachner M (2003) Tenascin-R-deficient mice show structural alterations of symmetric perisomatic synapses in the CA1 region of the hippocampus. *J Comp Neurol* 456: 338-349.
- Orend G (2005) Potential oncogenic action of tenascin-C in tumorigenesis. *The International Journal of Biochemistry and Cell Biology* 37: 1066-1083.
- Packard MG, Knowlton BJ (2002) Learning and memory functions of the Basal Ganglia. *Annu Rev Neurosci* 25:563-93. Epub; 2002 Mar 27.: 563-593.
- Pesheva P, Spiess E, Schachner M (1989) J1-160 and J1-180 are oligodendrocyte-secreted nonpermissive substrates for cell adhesion. *J Cell Biol* 109:1765-1778.
- Pesheva P, Gennarini G, Goridis C, Schachner M (1993) The F3/F11 cell adhesion molecule mediates the repulsion of neurons by the extracellular matrix glycoprotein J1-160/180. *Neuron* 10: 69-82.
- Pesheva P, Probstmeier R, Skubitz A, McCarthy JB, Furcht LT, Schachner M (1994) Tenascin-R (J1-160/180) inhibits fibronectin-mediated cell adhesion-functional relatedness to tenascin-C. *J Cell Sci* 107: 2323-2333.
- Pesheva P, Gloor S, Schachner M, Probstmeier R (1997) Tenascin-R is an intrinsic autocrine factor for oligodendrocyte differentiation and promotes cell adhesion by a sulfatide-mediated mechanism. *J Neurosci* 17(12): 4642-4651.
- Saga Y, Yaga T, Ikawa Y, Sakakura T, Aizawa S (1992) Mice develop normally without tenascin. *Genes Dev* 6: 1821-1831.
- Saghatelian AK, Gorissen S, Albert M, Hertlein B, Schachner M, Dityatev A (2000) The extracellular matrix molecule tenascin-R and its HNK-1 carbohydrate modulate perisomatic inhibition and long-term potentiation in the CA1 region of the hippocampus. *Eur J Neurosci* 12: 3331-3342.
- Saghatelian AK, Dityatev A, Schmidt S, Schuster T, Bartsch U, Schachner M (2001) Reduced perisomatic inhibition, increased excitatory transmission, and impaired long-term potentiation in mice deficient for the extracellular matrix glycoprotein tenascin-R. *Mol Cell Neurosci* 17(1): 226-240.

Schachner M (1994) Neural recognition molecules in disease and regeneration. *Curr Opin Neurobiol* 4: 726-734.

Schachner M, Taylor J, Bartsch U, Pesheva P (1994) The perplexing multifunctionality of janusin, an tenascin-related molecule. *Perspect on Dev Neurobiol* 2(1): 33-41.

Schumacher S, Jung M, Nörenberg U, Dorner A, Chiquet-Ehrismann R, Stuermer CAO, Rathjen FG (2001) CALEB binds via its acidic stretch to the fibrinogen-like domain of tenascin-C or tenascin-R and its expression is dynamically regulated after optic nerve lesion. *J Biol Chem* 276(10): 7337-7345.

Schumacher S, Stübe EM (2003) Regulated binding of the fibrinogen-like domains of tenascin-R and tenascin-C to the neural EGF family member CALEB. *J Neurochem* 87: 1213-1223.

Sotelo C (2004) Cellular and genetic regulation of the development of the cerebellar system. *Prog Neurobiol* 72: 295-339.

Srinivasan J, Schachner M, Catterall WA (1998) Interaction of voltage-gated sodium channels with the extracellular matrix molecules tenascin-C and tenascin-R. *Proc Natl Acad Sci USA* 95: 15753-15757.

Taylor J, Pesheva P, Schachner M (1993) Influence of Janusin and Tenascin on growth cone behavior *in vitro*. *J Neurosci Res* 35: 347-362.

Tepper JM, Bolam JP (2004) Functional diversity and specificity of neostriatal interneurons. *Curr Opin Neurobiol* 14: 685-692.

Teramoto T, Qiu J, Plumier JC, Moskowitz MA (2003) EGF amplifies the replacement of parvalbumin-expressing striatal interneurons after ischemia. *J Clin Invest* 111: 1125-1132.

Trepel (1995) *Neuroanatomie – Struktur und Funktion*. Urban & Schwarzenberg 1. Auflage: 137-153, 180-185.

Weber P, Bartsch U, Rasband MN, Czaniera R, Lang Y, Bluethmann H, Margolis RU, Rock Levinson S, Shrager P, Montag D, Schachner M (1999) Mice deficient for tenascin-R display alterations of the extracellular matrix and decreased axonal conduction velocities in the CNS. *J Neurosci* 19(11): 4245-4262.

Wintergerst ES, Fuss B, Bartsch U (1993) Localization of janusin mRNA in the central nervous system of the developing and adult mouse. *Eur J Neurosci* 5: 299-310.

Wolf HK, Buslei R, Schmidt-Kastner R, Schmidt-Kastner PK, Pietsch T, Wiestler OD, Blümcke I (1996) NeuN: A useful neuronal marker for diagnostic histopathology. *J Histochem Cytochem* 44(10): 1167-1171.

Woodworth A, Fiete D, Baenziger JU (2002) Spatial and temporal regulation of Tenascin-R glycosylation in the cerebellum. *J Biol Chem* 277(52): 50941-50947.

Xiao ZC, Bartsch U, Margolis RK, Rougon G, Montag D, Schachner M (1997) Isolation of a tenascin-R binding protein from mouse brain membranes: a phosphacan-related chondroitin sulphate proteoglycan. *J Biol Chem* 272(51): 32092-32101.

Xiao ZC, Ragsdale DS, Malhotra JD, Mattei LN, Braun PE, Schachner M, Isom LC (1999) Tenascin-R is a functional modulator of sodium channel β subunits. *J Biol Chem* 274(37): 26511-26517.

Yamanaka H, Yanagawa Y, Obata K (2004) Development of stellate and basket cells and their apoptosis in mouse cerebellar cortex. *Neurosci Res* 50: 13-22.

Zhou FM, Wilson CJ, Dani JA (2002) Cholinergic interneuron characteristics and nicotinic properties in the striatum. *J Neurobiol* 53: 590-605.

8 ABBREVIATIONS:

%	per cent
°	degree
°C	Grade Celsius
α	alpha
AEP	auditory evoked potentials
β	beta
β1,4-linked GalNAc-4-SO ₄	sulphated carbohydrate structure
CA1	region in the hippocampus
Ca ²⁺	Calcium
CaCl ₂	Calcium chloride
CALEB	chicken acidic leucine-rich EGF-like domain containing brain protein
ChAT	choline acetyltransferase (a specific marker for a subpopulation of inhibitory interneurons in the striatum)
CNS	central nervous system
CSPG	chondroitin sulphate proteoglycan
Cy3	Carbocyanine 3 (red fluorescentcarbocyanine)
CNP	cyclic nucleotide phosphodiesterase
ECM	Extracellular Matrix
EEG	electroencephalogram
e.g.	exempli gratia, for example
EGF	epidermal growth factor
F3/F11	a cell surface receptor
FN	fibronectin
g	gram
GABA	γ-amino-butric-acid
GFAP	glial fibrillary acidic protein
HNK-1	α 3`-sulphated glucuronic acid
Hz	Hertz

Iba-1	macrophage/microglia-specific calcium-binding protein
i.e.	in example
Ig	Immunoglobulin
Ig G	Immunoglobulin G
IPSC	inhibitory postsynaptic currents
J1-160/180	old name of Tenascin-R
J1-160	old name of the 160kD isoform of Tenascin-R
J1-180	old name of the 180kD isoform of Tenascin-R
kD	kilo Dalton
ko	knockout
l	litre
LTP	long-term potentiation
μ	micro (10^{-6})
μm	micrometre
M	Molar
m	milli (10^{-3})
mm	millimetre
mm^3	cubic millimetre
Mo	month
mRNA	messenger ribonucleic acid
n	nano (10^{-9})
NaOH	Sodiumhydrogencarbonate
NeuN	anti neuron specific nuclear antigen
NMDA	<i>n</i> -methyl-D-aspart
Mac-1	marker for microglia
P	postnatal day
PBS	phosphate buffered saline
PCR	polymerase chain reaction
PV	Parvalbumin
RT	room temperature
SD	standard difference
SPF	specific pathogen-free

SPSS	Sigma Plot 8 software
S-100	low molecular weight calcium-binding protein expressed in astrocytes
TA	tenascin assembly
TN-C	Tenascin-C
TN-R	Tenascin-R
TN-R+/+	wild-type mouse
TN-R-/-	Tenascin-R deficient mouse
TN-W	Tenascin-W
TN-X	Tenascin-X
TN-Y	Tenascin-Y
UKE	Universitätsklinikum Hamburg
w/v	weight per volume
x	dimension in the room
y	dimension in the room
z	dimension in the room

9 ACKNOWLEDGMENTS

I am grateful to Prof. Dr. M. Schachner for the possibility to carry out the academic investigation to write this dissertation and for the nice support.

I would like to thank Dr. Andrey Irintchev for the nice support and that I could ask him my questions every time.

Thank you to Emanuela Szpotowicz for the given assistance with the preparation of the mice and the staining of the sections.

I want to say thank you to all people in my lab and to all people in the institute for the friendly integration and for answering my questions, explaining the microscope to me and helping me with the computer.

And I want to thank my family for the nice support.

10 CURRICULUM VITAE

Family name	Steen
First name	Ann-Britt
Date of birth	March 3 rd 1980
Place of birth	Stade, Germany
Nationality	German
Confession	Evangelic Lutheran
Marital status	single

Education

08/86 – 07/89	Grundschule am Wingster Wald, Wingst
08/89 – 07/90	Grundschule Cadenberge, Cadenberge
08/90 – 07/92	Orientierungsstufe, Cadenberge
08/92 – 07/99	Gymnasium Warstade, Hemmoor
	Graduation: Allgemeine Hochschulreife

University

Since 04/00	Regular student of medicine, University of Hamburg
-------------	-------------------------------------------------------

Exams

03/02	Physikum
03/03	1. Staatsexamen
03/05	2. Staatsexamen
04/06	3. Staatsexamen

Dissertation

Since 08/03	Quantitative Morphological Analyses of the Striatum and Cerebellum of Tenascin – R – deficient mice, Zentrum für Molekulare Neurobiologie Hamburg, Institut für Biosynthese Neuraler Strukturen, Prof. Dr. Schachner
-------------	----------------------------------------------------------------------------------------------------------------------------------------------------------------------------------------------------------------------------

11 EIDESSTATTLICHE VERSICHERUNG

Ich versichere ausdrücklich, dass ich die Arbeit selbständig und ohne fremde Hilfe verfasst, andere als die mir angegebenen Quellen und Hilfsmittel nicht benutzt und die aus den benutzten Werken wörtlich oder inhaltlich entnommenen Stellen einzeln nach Ausgabe (Auflage und Jahr des Erscheinens), Band und Seite des benutzten Werkes kenntlich gemacht habe.

Ferner versichere ich, dass ich die Dissertation bisher nicht an einen Fachvertreter an einer anderen Hochschule zur Überprüfung vorgelegt oder mich anderweitig um Zulassung zur Promotion beworben habe.

Unterschrift: